JOHNSON MATTHEY
TECHNOLOGY REVIEW
www.technology.matthey.com

Johnson Matthey Highlights

A selection of recent publications by Johnson Matthey R&D staff and collaborators

Activity of Molybdenum and Tungsten Oxycarbides in Hydrodenitrogenation of Carbazole Leading to Isomerization Secondary Reaction of Bicyclohexyl. Results Using Bicyclohexyl as Feedstock

M. Lewandowski, A. Szymańska-Kolasa, C. Sayag and G. Djéga-Mariadassou, *Appl. Catal. B: Environ.*, 2020, **261**, 118239

Bulk W and Mo oxycarbides were synthesised and characterised by a range of physicochemical techniques. The catalytic behaviour of the oxycarbides was tested for the carbazole hydrodenitrogenation (HDN) and the bicyclohexyl (BCH) isomerisation reactions. High isomerisation catalytic activity was demonstrated for both oxycarbides. The addition of 50 ppm of sulfur increased this activity further during the HDN of carbazole. W_2C demonstrated the highest catalytic activity for both pure BCH isomerisation and secondary BCH isomerisation during the HDN of carbazole. Ethylbicyclo[4.4.0]decane (an isomerisation product) and *n*-hexylcyclohexane (a ring opening product) were the main BCH isomers detected for both oxycarbides. The presence of these products, in significant quantities, indicated that the bulk oxycarbides are bifunctional catalysts with both acid and metallic sites.

Solid State NMR Service Across the World

N. S. Barrow and P. Jonsen, *Solid State Nucl. Magn. Reson.*, 2020, **105**, 101626

24 global SSNMR laboratories were interviewed on the telephone and face-to-face in early 2019. Data was collected related to service throughput, staff, barriers and equipment. The hardware profile observed in this study agreed with a previous report published in 2013 which primarily looked at SSNMR in the UK. This study highlights that a lack of knowledge about SSNMR capabilities is the biggest barrier. By conducting this research, a strong benchmark has been set. SSNMR laboratories can therefore identify their barriers and implement changes to maximise the use of SSNMR within their own research.

Correlating Physicochemical Properties of Commercial Membranes with CO_2 Absorption Performance in Gas-Liquid Membrane Contactor

Y. Xu, C. Malde and R. Wang, *J. Membr. Sci. Res.*, 2020, **6**, (1), 30

Polypropylene (PP) and polyvinylidene fluoride (PVDF) hollow fibre membranes were applied to investigate the impact of their physicochemical properties on long-term CO_2 absorption performance in a gas-liquid membrane contactor (GLMC). CO_2 transport was hindered by membrane wetting and fouling when water was used as an absorbent, which resulted in continuous flux during long-term operation. When monoethanolamine (MEA) was used as an absorbent, both PP and PVDF membranes demonstrated dramatic flux decline. The pore size, stability, morphology and hydrophobicity of commercial membranes were shown to be affected by MEA over long-term operations. Therefore, the authors propose selection criterion of microporous membranes.

Implications of the Molybdenum Coordination Environment in MFI Zeolites on Methane Dehydroaromatisation Performance

M. Agote-Arán, R. E. Fletcher, M. Briceno, A. B. Kroner, I. V. Sazanovich, B. Slater, M. E. Rivas, A. W. J. Smith, P. Collier, I. Lezcano-González and A. M. Beale, *ChemCatChem*, 2020, **12**, (1), 294

In situ XAS and DFT were used to compare the structure and activity of Mo/Silicalite-1 (Si:Al = ∞) to Mo/H-ZSM-5 (Si:Al = 15). Calcination in Mo/Silicalite-1 was shown to disperse the MoO_3 precursor into tetrahedral Mo-oxo species, in close proximity to the microporous framework. Both catalysts were shown to be active for methane dehydroaromatisation (MDA). Mo/Silicalite-1 demonstrated faster sintering of the Mo species, which led to rapid deactivation. This contributed to the accumulation of carbon deposits on the zeolite outer surface. Thus, this study highlights the importance of framework Al for the stabilisation of active Mo species, when under MDA conditions.

Strength and Fragmentation Behaviour of Complex-Shaped Catalyst Pellets: A Numerical and Experimental Study

A. Farsi, J. Xiang, J. P. Latham, M. Carlsson, E. H. Stitt and M. Marigo, *Chem. Eng. Sci.*, 2020, **213**, 115409

The relationship between catalyst support shape and final strength and fragmentation behaviour was investigated. Pellet crushing behaviours were examined by performing uniaxial compression tests on solid and four-holed discs (**Figure 1**). The finite-discrete element method (FDEM) was used to provide a detailed analysis of the fragmentation evolution of pellets. The FDEM method also revealed a primary failure undetected in laboratory tests. Concentration of compressive stress in the pellet core led to a greater fraction of fines and the choking effect of these fines contributed to pressure drops. These drops had a greater impact on fixed-bed reactors made with solid cylindrical catalysts than to those made with four-holed catalyst supports.

Structure and Ion Transport of Lithium-Rich $Li_{1+x}Al_xTi_{2-x}(PO_4)_3$ with $0.3<x<0.5$: A Combined Computational and Experimental Study

D. Case, A. J. McSloy, R. Sharpe, S. R. Yeandel, T. Bartlett, J. Cookson, E. Dashjav, F. Tietz, C. M. N. Kumar and P. Goddard, *Solid State Ionics*, 2020, **346**, 115192

In this experimental and computational study, the structural sensitivities of $Li_{1+x}Al_xTi_{2-x}(PO_4)_3$ with $0.3 < x < 0.5$ were examined by modelling the site occupancies at varying temperatures. Li-ion transport properties were reported computationally for the first time. Simulations demonstrated that only the M1(6b) and M2(18e) sites were involved in the migration pathway, which aligned with the neutron diffraction data. Low migration barriers (0.3 eV) were calculated in agreement with experimental findings. Experimentally, no improved Li-ion conductivity was observed above $x = 0.3$ and this could be explained by Li-ion trapping on Al doping where $x = 0.4$.

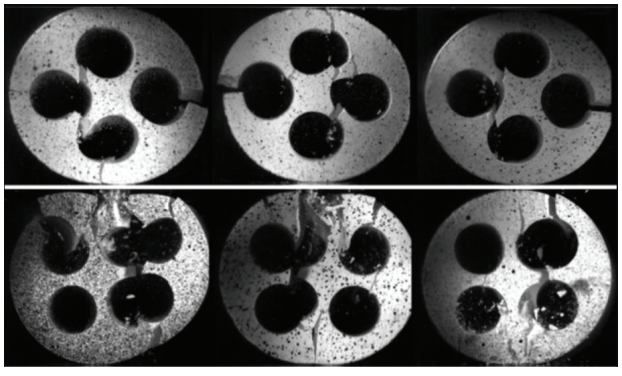

Fig. 1. Reprinted from A. Farsi *et al.*, *Chem. Eng. Sci.*, 2020, **213**, 115409, Copyright (2020), with permission from Elsevier

Flow and Forced Convection Heat Transfer Characteristics of Developed Laminar Flow in the Octahedral Channels of Octo-Square Asymmetric Particulate Filters

T. C. Watling, *Res. Eng.*, 2020, **5**, 100086

Octahedral channels are present in octo-square asymmetrical diesel and gasoline particulate filters. In this study, the flow and forced convection heat transfer characteristics of these channels were investigated. Least squares and point matching methods were employed to determine the temperature and velocity fields, with the least squares method being the most effective. The viscous loss coefficient and the product of the channel perimeter and heat transfer coefficient decreased as the channel cross section became closer to a regular octahedron, whereas the friction factor and Nusselt number were shown to increase. When comparing an octahedral channel and a square channel of the same width, there was minimal difference between the heat transfer and along-channel pressure drop.

PBI Mixed Matrix Hollow Fiber Membrane: Influence of ZIF-8 Filler over H_2/CO_2 Separation Performance at High Temperature and Pressure

M. Etxeberria-Benavides, T. Johnson, S. Cao, B. Zornoza, J. Coronas, J. Sanchez-Lainez, A. Sabetghadam, X. Liu, E. Andres-Garcia, F. Kapteijn, J. Gascon and O. David, *Sep. Purif. Technol.*, 2020, **237**, 116347

A scalable hollow fibre spinning process was used to develop high performance mixed-matrix membranes for H_2/CO_2 separation. The membranes were able to operate up to 30 bar at 150ºC. A ZIF-8 filler was used which contributed to a 65% increase in H_2 permeance at constant ideal selectivity. Competition was observed between H_2 and CO_2 transport inside the ZIF-8 structure for mixed gas permeation. The adsorption of CO_2 in the nanocavities of the ZIF-8 filler suppressed the transport of H_2, which led to a decrease in H_2 permeance. The mixed gas performance was compromised at high operating feed pressures.

Measuring Velocity and Turbulent Diffusivity in Wall-Flow Filters Using Compressed Sensing Magnetic Resonance

J. D. Cooper, A. P. E. York, A. J. Sederman and L. F. Gladden, *Chem. Eng. J.*, 2019, **377**, 119690

Recirculating flows and turbulent diffusivity in wall-flow particulate filters were observed for the first time using gas-phase compressed sensing magnetic resonance (MR) methods. Entrance and exit gas flow distributions were characterised using 2D MR velocity imaging. Fast 3D compressed sensing MRI was used to quantify turbulent diffusivity. Contrary to numerical predictions, the

data collected demonstrated that different regions of turbulent diffusivity were present within the filter. For instance, at the entrance, two different regions of turbulent diffusivity were observed, both within the inlet channels.

Synthesis and Characterization of $LiFe_{1-x}Mn_xPO_4$ (x = 0.25, 0.50, 0.75) Lithium Ion Battery Cathode Synthesized *via* a Melting Process

E. B. Fredj, S. Rousselot, L. Danis, T. Bibienne, M. Gauthier, G. Liang and M. Dollé, *J. Energy Storage*, 2020, **27**, 101116

Melt synthesis, a low-cost and simple method, was used to synthesise electrochemically active $LiFe_{1-x}Mn_xPO_4$ (x = 0.25, 0.50, 0.75) cathode materials for the first time. SEM, XRD and galvanostatic charge/discharge cycling were used to characterise the $LiFe_{1-x}Mn_xPO_4$ materials. Results were compared to those of solid-state synthesised materials. Overall, capacity retention, rate capability and discharge capacity were similar for both materials. However, melt synthesised $LiFe_{0.25}Mn_{0.75}PO_4$ had a higher capacity than solid-state synthesised $LiFe_{0.25}Mn_{0.75}PO_4$. Therefore, melt synthesis could offer a viable alternative to current synthetic techniques.

Understanding the Mechanochemical Synthesis of the Perovskite $LaMnO_3$ and its Catalytic Behaviour

R. H. Blackmore, M. E. Rivas, T. E. Erden, T. D. Tran, H. R. Marchbank, D. Ozkaya, M. Briceno de Gutierrez, A. Wagland, P. Collier and P. P. Wells, *Dalton Trans.*, 2020, **49**, (1), 232

Lanthanum manganite was synthesised from metal oxide powders (Mn_2O_3 and La_2O_3) *via* mechanochemistry using a planetary ball mill. During the milling process, 'time slices' were taken. 100% perovskite phase was observed after 3 h of milling, as derived from XRD analysis. However, results from XAS analysis demonstrated that significant structural alterations took place after just 30 min. XAS also highlighted the presence of amorphous, oxygen deficient, content. Increased oxygen deficiency at the surface led to the $LaMnO_3$ catalyst displaying early onset production of N_2 (in comparison to sol-gel synthesised $LaMnO_3$). Therefore, mixed metal oxide catalysts with enhanced catalytic properties can be prepared *via* mechanochemical routes.

Influence of Synthesis Conditions on the Structure of Nickel Nanoparticles and their Reactivity in Selective Asymmetric Hydrogenation

R. Arrigo, S. Gallarati, M. E. Schuster, J. M. Seymour, D. Gianolio, I. da Silva, J. Callison H. Feng, J. E. Proctor, P. Ferrer, F. Venturini, D. Grinter and G. Held, *ChemCatChem*, 2020, **12**, (5), 1491

A hot-injection colloidal route was used to synthesise unsupported and silica-supported Ni NPs. NP size and Ni electronic structure were affected by changing equivalents of reducing and protective agents. (*R,R*)-Tartaric acid (TA) was used to modify the NPs which were then investigated in the asymmetric hydrogenation of methyl acetoacetate to chiral methyl-3-hydroxy butyrate. A Ni metallic active surface was identified where activity was shown to increase with metallic domain size. Particle size had no impact on selectivity for unsupported NPs. Catalysts that contained positively charged Ni species demonstrated very high (*R*)-selectivity. At long reaction times, TA modification of metallic Ni NPs was shown to be unsatisfactory for the maintenance of high (*R*)-enantiomer selectivity.